Applied Catalysis B: Environmental 164 (2015) 334–343

Contents lists available at ScienceDirect

Applied Catalysis B: Environmental

journal homepage: www.elsevier.com/locate/apcatb

Insight into effect of acid/base nature of supports on selectivity of glycerol oxidation over supported Au-Pt bimetallic catalysts

Chunli Xu[a,b,*], Yuqun Du[a,b], Chao Li[c], Jun Yang[a,b], Guang Yang[c]

[a] Key Laboratory of Applied Surface and Colloid Chemistry (Shaanxi Normal University), Ministry of Education, Xi'an710119, PR China
[b] School of Chemistry and Chemical Engineering, Shaanxi Normal University, Chang'an West Street 620, Xi'an 710119, PR China
[c] Electronic Materials Research Laboratory, Key Laboratory of the Ministry of Education & International Center for Dielectric Research, Xi'an Jiaotong University, Xi'an 710049, PR China

ARTICLE INFO

Article history:
Received 28 May 2014
Received in revised form 20 August 2014
Accepted 22 September 2014
Available online 28 September 2014

Keyword:
Oxidation of glycerol
Solid acid
Catalysis
Gold
Solid bases

ABSTRACT

Au-Pt bimetallic catalysts were supported on different supports, including acidic (TiO_2 and CeO_2), basic (MgO, $Mg(OH)_2$, $(MgCO_3)_4Mg(OH)_2$, ZnO, and $CaCO_3$), and amphoteric (Al_2O_3 and hydrotalcite) supports with the aim to study the effect of the acid/base properties of supports upon the performance of Au-Pt bimetallic catalysts in glycerol oxidation. The results showed that these properties significantly affected the selectivity of products. The selectivity to glyceraldehyde was inversely proportional to the strength of supports' basic sites, and the selectivity to tartronic acid (or glycolic acid, or glyoxalic acid) was proportional to the strength of basic sites. In contrast, the selectivity to glyceric acid was neither proportional to the strength of basic sites nor proportional to the strength of acid sites. The doping of another weaker basic site also affected the selectivity to glyceric acid. Furthermore, the role of the acid/base nature of the supports in affecting the products' distribution is proposed.

1. Introduction

Much attention has been given to the transformation of biomass and biomass-derived chemicals to fuel and valuable chemicals for sustainable development [1,2]. The oxidation of several classes of alcohols, including monoalcohols, 5-hydroxymethylfurfural and polyols, is an important research topic in the transformation of biomass [3]. The polyol glycerol is a byproduct of the transesterification of vegetable oil and animal fats into biodiesel. Thus, the oxidation of glycerol to fine chemicals might help offset the cost of biodiesel production [4,5]. Academic interest in oxidative upgrading of glycerol stems from glycerol being a model polyol with three hydroxyl groups [5]. Traditional methods for oxidation have utilized organic solvents or inorganic oxidants such as transition metal oxo compounds, halogenated compounds and sulfur oxides [6,7]. Use of metal catalysts during oxidation in liquid water with molecular oxygen provides a sustainable and economical route for alcohol oxidation [7]. Glycerol contains two primary OH groups and one secondary OH group. The oxidation of glycerol has a complex reaction pathway (Scheme 1) [5]. Theoretically, six potential C_3 oxygenated products: dihydroxyacetone (DHA), hydroxypyruic acid (HPYA), mesoxalic acid, glyceraldehyde (GLYALD), glyceric acid (GLYA), tartronic acid (TARAC), together with C_2 (oxalic acid (OXALA), glycolic acid (GLYCA), glyoxylic acid (GA)) and C_1 products (formic acid (FORM), COx), can be obtained. Selective vs. non-selective oxidation is a challenge associated with these possible catalytic oxidation reactions [8]. Heterogeneous catalysts play a key role in the promotion and control of such reactions. Hence, the first important step in the industrialization of any new process requires the design of new effective heterogeneous catalysts to control the chemoselective direction of the glycerol oxidation reaction.

The oxidation of glycerol has been intensively investigated using monometallic metal catalysts, such as Au, Pt and Pd [5]. A key advantage in using gold, as compared to Pt and Pd, is the improved resistance of Au to overoxidation under liquid-phase oxidation conditions with O_2 as the oxidant [9]. However, in alcohol oxidation with gold catalysts, a severe limitation arises because of the necessary addition of a homogeneous base to improve the oxidation kinetics and reduce deactivation [9]. Without the addition of a homogeneous base, such as NaOH, there is no glycerol conversion over Au/C catalysts [10]. The addition of homogeneous base presents negative environmental and economic impacts since the high pH of the medium in corrosive and the salts of product need

* Corresponding author at: School of Chemistry and Chemical Engineering, Shaanxi Normal University, 620 Chang'an West Street, Xi'an 710119, PR China. Tel.: +86 29 81530779.
E-mail address: xuchunli@snnu.edu.cn (C. Xu).

http://dx.doi.org/10.1016/j.apcatb.2014.09.048
0926-3373/

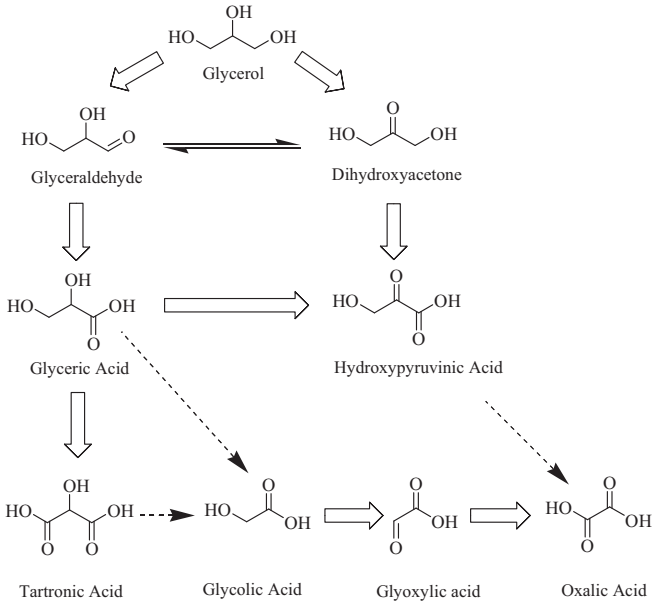

Scheme 1. Reaction pathway for glycerol oxidation [5].

to be neutralized to release free acid [5]. A major topic of current research on glycerol oxidation is the performance of bimetallic catalysts [5]. In the absence of base, bimetallic catalysts show higher conversion than monometallic Au, Pd or Pt catalysts. Furthermore, the application of bimetallic catalysts could solve the limitations arising from the addition of homogeneous bases. A Pd-Au/C catalyst was explored in the absence of base for glycerol oxidation by Prati et al. [11]. A higher conversion of 11.9% for the 1% Pd-Au(1:1)/C catalyst, compared to 3% conversion for the monometallic 5% Pd/C catalyst, was reported after 1 h at 353 K. In the absence of base at the relatively higher temperature (373 K), Villa et al. [9] observed only 5% conversion of glycerol and 70% selectivity to GLYA over a monometallic 1% Au/H-mordenite catalyst, but 70% conversion of glycerol and 83% selectivity to GLYA over a bimetallic 1% (Au:Pt 6:4)/H-mordenite. Brett et al. [12] also investigated the effect of bimetallic Au-Pt and Au-Pd supported on MgO in the absence of added base. They observed 42.5% conversion of glycerol and 85.1% selectivity to GLYA over a bimetallic 1% Au-Pt(1:3)/MgO after 24 h at ambient temperature. More recently, Tongsakul et al. [13] explored hydrotalcite (HT)-supported Au-Pt alloy nanoparticles using a soluble starch as a green reductant and stabilizing agent. They found 73% conversion of glycerol and 78% selectivity to GLYA over a $Pt_{60}Au_{40}$–starch/HT catalyst after 6 h at ambient temperature. In these studies relating to bimetallic catalysts, supports with various acid/base properties have been applied, including basic supports (MgO) [12], amphoteric supports (HT) [13], acid supports (H-mordenite) [9], and neutral supports (carbon) [11]. One question arising from the bimetallic catalysis was the effect of the acid/base properties of supports upon the conversion and selectivity of glycerol oxidation. For the monometallic catalysts, such as Au, Pt and Pd, both the conversion of glycerol and selectivity of products were affected by the addition of homogeneous base [5]. Even in the presence of homogeneous base, the acid/basic property of supports also affects the activity and selectivity of monometallic catalysts [14]. However, for bimetallic catalysis, it is not clear how the nature of the supports affects their catalytic properties. Clarification of the role of the nature of supports is therefore instructive to design high activity and selective bimetallic catalysts [5,15,16].

In this work, various supports, including acid, basic, and amphoteric supports, were studied, with the aim of studying the effect of acidity/basicity upon the selectivity of Au-Pt bimetallic catalysts in the glycerol oxidation. This study concentrates upon three supports, HT, MgO, and γ-Al_2O_3. In order to further understand the role of acid/basic property of supports, a series of reference supports (TiO_2, CeO_2, $Mg(OH)_2$, $(MgCO_3)_4Mg(OH)_2$, ZnO, and $CaCO_3$) was also investigated.

2. Experimental

2.1. Catalyst preparation

2.1.1. Preparation of supports

HT support was prepared using a standard aqueous co-precipitation method, as described in our previous report [17]. An aqueous solution (300 mL) of the metal nitrates in a Mg^{2+}:Al^{3+} molar ratio of 5:1 with a total concentration of 1.5 M was mixed slowly with continuous stirring with an alkaline solution of Na_2CO_3-NaOH. The molar amount of Na_2CO_3 used was twice that of Al^{3+}. The pH of the mixture was kept constant, typically at values between 9 and 10, by adjusting the flow rate of the alkaline solution. The temperature was maintained at 25 °C. Following this addition, which resulted in the formation of a heavy slurry, the mixture was aged at 60 °C for 18 h with stirring, to facilitate the selective growth of the precipitated HT phase. The slurry was then cooled to 25 °C, filtered, and washed with water until the pH value of the filtrate was around 7. The precipitate was dried at 90 °C for 16 h. The resulting material was HT.

Mesoporous MgO as support for gold catalyst was prepared by calcining $Mg(OH)_2$ sample (AR, 99%, Guangdong Shantou Hongwei Chemical plant, P.R. China) at 400 °C for 3 h in static air (muffle oven, heating rate: 10 °C min^{-1}). γ-Al_2O_3 support was prepared by calcining γ-Al_2O_3 (a commercial sample, Alfa Aesar) at 500 °C for 3 h in static air.

A series of other commercially available supports were used as received without any pretreatment. The used supports were as follows: ZnO (AR, 99%, Xi'an Chemical Reagent Plant, China), CeO_2 (UP, 99.99%, Sinopharm Chemical Reagent Co., Ltd, China), $CaCO_3$ (AR, 99%, Shanghai Fengxian Fengcheng Reagent Plant, China), $(MgCO_3)_4Mg(OH)_2 5H_2O$ (AR, MgO 40.0–44.5%, Sinopharm Chemical Reagent Co., Ltd, P.R. China), and TiO_2 (P25, AR, Beijing Technology & Trade Co., Ltd. Ante Pune, China).

2.1.2. Synthesis of the gold supported catalyst

Supported 1 wt% Au-Pt catalysts were prepared using a sol-immobilisation method [12]. Aqueous solutions of $H_2PtCl_6 \cdot 6H_2O$ and $HAuCl_4 \cdot 4H_2O$ of the desired concentration were prepared. To this solution polyvinyl alcohol (PVA) (weight-average molecular mass = 9000–10,000 g/mol) was added such that the PVA to Au-Pt ratio was 0.5 by mass. Subsequently, a freshly prepared 0.1 M solution of $NaBH_4$ (>96% purity, $NaBH_4$/metal mole fraction = 5) was added to form a dark-brown sol. After 30 min of sol–gel generation, the colloid was immobilized by adding a support under vigorous stirring. The amount of support material required was calculated to give a final metal loading of 1 mass%. In order to make sure gel adsorbed on supports completely, the pH value of gel was adjusted to be less than the isoelectric point of the corresponding supports (Table S1). After 2 h, the slurry was filtered, the catalyst washed thoroughly with distilled water and dried at 110 °C overnight. Further catalysts were prepared using a different mole fraction of Au:Pt.

2.2. Characterization of catalyst

The surface area and pore characteristics of the catalysts were determined using a Micromeritics ASAP 2020 instrument (America). The sample was degassed at different temperatures (100 °C for HT, 250 °C for oxide) for 4 h in N_2 prior to surface

area measurements. Nitrogen adsorption and desorption isotherms were measured at −196 °C, and the specific surface areas of the catalysts were determined by applying the BET (Brunauer–Emmett–Teller) method to the nitrogen adsorption data obtained in the relative pressure range from 0.06 to 0.30. Total pore volumes were estimated from the amount of nitrogen adsorbed at a relative pressure of 0.995. Pore volume and pore size distributions were obtained from analysis of the desorption branches of the nitrogen isotherms using the BJH (Barrett–Joyner–Halenda) method.

X-ray diffraction (XRD) patterns were recorded on a D/Max-3C X-ray powder diffractometer (Rigaku Co, Japan), using a Cu-K source fitted with an Inel CPS 120 hemispherical detector.

Hammett indicator experiments were conducted to determine the acid/basic strength of each catalyst support. The Hammett indicators used were methyl yellow ($pK_a = 3.3$), methyl red ($pK_a = 4.8$), neutral red ($pK_a = 6.8$), bromothymol blue ($pK_a = 7.2$), phenolphthalein ($pK_a = 9.8$), alizarin yellow R ($pK_a = 11.0$), indigo carmine ($pK_a = 12.2$), 2,4-dinitroaniline ($pK_a = 15$), 4-nitroaniline ($pK_a = 18.4$), and 4-chloroaniline ($pK_a = 26.5$). Typically, 0.1 g of the catalyst support was mixed with 2 mL of a solution of Hammett indicators diluted with distilled water and left for 2 min. After the equilibration, the color of the support was noted. The acid/basic strength of the support was taken to be higher than the weakest indicator that underwent a color change and lower than the strongest indicator that underwent no color change. The acid strength was denoted H_o, and the basic strength was denoted H_-.

The gold loading of the catalysts was determined by flame atomic absorption spectrometry. A TAS986 atomic absorption spectrophotometer was used, the wavelength range detected was 190–900 nm. A hollow cathode lamp of gold and platinum (Ningqiang Source, Hengshui, China) was used as radiation source at 5.0 mA. The analytical line at 242.8 nm (Au) and 265.9 nm (Pt) was used in the measurements with 0.4 nm as the spectral bandwidth.

In order to elucidate the microstructure and compositions of Au-Pt nanoparticles, a scanning transmission electron microscopy (STEM) with energy dispersive X-ray spectroscopy (EDS) was used (a JEOL ARM200F microscope equipped with probe Cs corrector).

X-ray photoelectron spectra (XPS) were used to characterize the basic sites of catalysts. XPS were obtained in an AXIS ULTRA spectrometer (Kratos Analytical Ltd., Japan) using AlKα ($h\upsilon = 1486.6$ eV) X-ray radiation at an energy of 150 W. Spectra were collected at room temperature and at a pressure in the analyzer chamber of 5×10^{-9} Torr. Photoelectron kinetic energies were measured with a hemispherical energy analyzer working at constant pass energy of 50 eV. The binding energy scale was corrected by setting the C1s transition to 284.8 eV.

2.3. Reaction procedure

The reaction tests were performed in a 100 mL stainless steel autoclaves (Parr autoclaves) equipped with manometers, temperature sensors, magnetic stirrers and sample outlets. The glycerol solution (0.3 mol/L, 15 mL) was admitted into the reactor and the desired amount of catalyst (glycerol/metal mole fraction = 1000) was added. The reactor was purged with oxygen three times and adjusted to the desired pressure of 300 kPa. The reaction mixture was heated to the desired temperature (60 °C) and stirred for the requisite amount of time (4 h). The reactor vessel was then cooled to room temperature and the reaction mixture was analyzed. This analysis was carried out using high-pressure liquid chromatography (HPLC) equipped with refractive index detectors. Samples of the reaction mixture (0.5 mL) were diluted (to 1 mL) using the eluent. Products were identified by comparison with authentic samples. For the quantification of the reactants consumed and products generated, an external calibration method was used.

Table 1
Nitrogen physisorption data of supports and catalysts.

Sample	Surface area[a] ($cm^2\ g^{-1}$)	Pore volume[b] ($cm^3\ g^{-1}$)	Pore diameter[b] (Å)
HT	43	0.28	214
Au-Pt/HT	45	0.30	161
MgO	243	0.49	64
Au-Pt/MgO	84	0.50	250
γ-Al_2O_3	188	0.56	119
Au-Pt/γ-Al_2O_3	195	0.53	77

[a] Calculated by the BET method.
[b] Calculated by the BJH method from the desorption isotherm.

As shown in the section above, the theoretical products of glycerol oxidation are various. The products observed by some of the famous groups were outlined in Table S2 [7,12,14,18–22]. Although the distribution of products depended on the property of catalysts, the main products were GLYA, TARAC, GLYCA, and OXALA. Beside Tsuji et al. [20] (Table S2, entry 5), the amount of GLYALD was either not reported or low (<4%; Table, entries 1 and 4). In this work, the observed products were GLYALD, GLYA, TARAC, GLYCA, GA, and OXALA. The diversity of products makes it difficult to separate them each other. In order to separate them, the involved chromatograph column were various, such as Zorbax SAX column (Table S2, entry 1) [18], HPX-87H (entries 2 and 5) [7,20], metacarb 67H (entry 3) [12], and Alltech OA-10308 (entry 7) [21]. The columns were different in their ability of separating products. In this work, HPX-87H column was used. It was found that HPX-87H column could not well separate GLYA from GLYALD using H_2SO_4 as mobile phase (entry 5) [20]. In order to well separate the products, two mobile phases were used. One was aqueous H_2SO_4, and the other was HCOOH (entry 9). Although HCOOH was the theoretical products of glycerol oxidation, the observed amount of HCOOH was low. The data about HCOOH in references also confirmed that HCOOH were not the main product of glycerol oxidation (Table S2). Furthermore, it was found that HCOOH of mobile phase could well separate GLYA from GLYALD. Therefore, H_2SO_4 eluent was used to separate glycerol, TARAC, GLYCA, GA, and OXALA; HCOOH eluent was used to separate GLYA from GLYALD.

3. Results and discussion

3.1. Catalyst characterization

3.1.1. BET surface area and pore size

As shown in Table 1, the surface area of HT was 43 $m^2\ g^{-1}$, which was far lower than that of MgO (243 $m^2\ g^{-1}$) and γ-Al_2O_3 (188 $m^2\ g^{-1}$). The pore size distribution of HT was far broader than that of the other two supports (Fig. 1). The isotherms of the three samples had the characteristic Type IV shape. The Type IV isotherm and pore size distribution suggested that the three samples were mesoporous materials. The surface area of Au-Pt/HT and Au-Pt/γ-Al_2O_3 were similar with their corresponding supports. However, the surface area of Au-Pt/MgO was far lower than that of its MgO support.

3.1.2. XRD analysis

Figs. 2–4 display the XRD patterns of supports and Au-Pt catalysts. The X-ray diffractograms of HT and Au-Pt/HT were similar, corresponded to typical X-ray diffractograms for HT (Fig. 2) [17]. The X-ray diffractograms of γ-Al_2O_3 and Au-Pt/γ-Al_2O_3 were also similar, showing the typical features of γ-Al_2O_3 (Fig. 4) [17]. This indicated that the crystalline structure of HT and γ-Al_2O_3 supports did not change after supporting the Au-Pt phase. The XRD patterns of MgO and Au-Pt/MgO are presented in Fig. 3. It can be seen that the major phase present for the MgO support was MgO, while

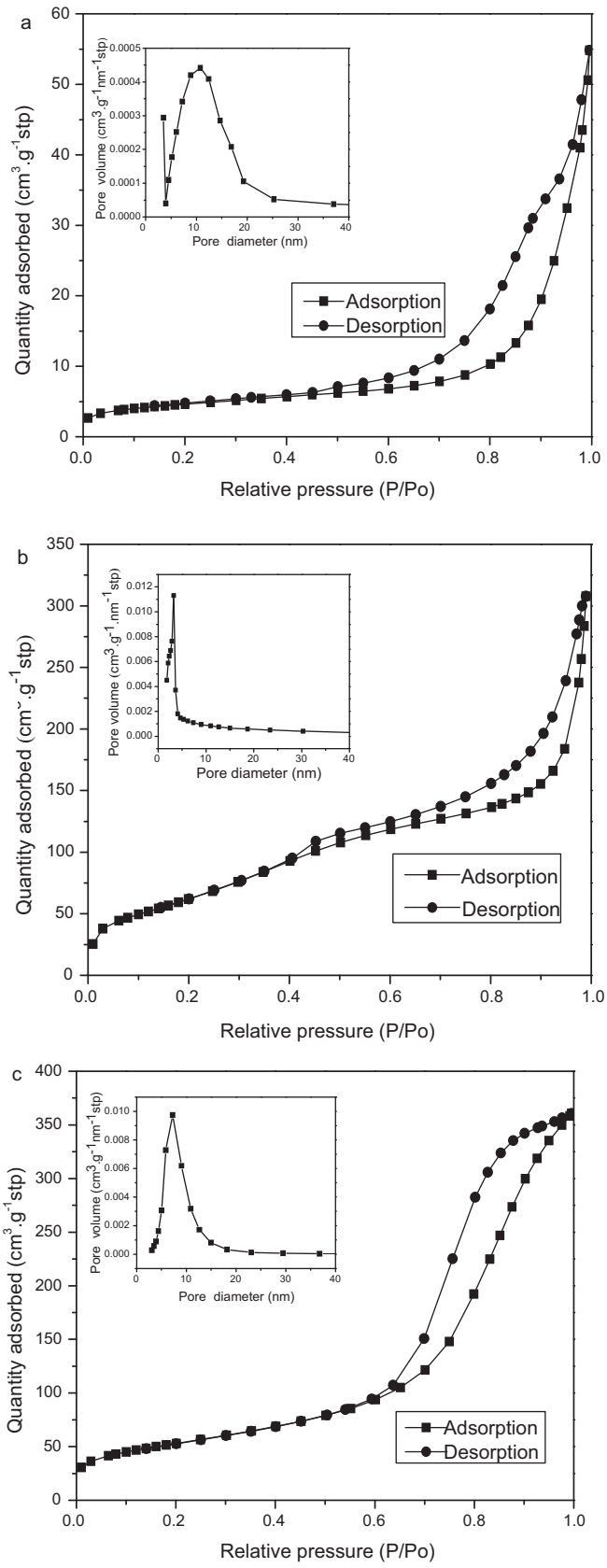

Fig. 1. Nitrogen physisorption isotherms (■, adsorption; ●, desorption) and BJH pore size distribution for (a) HT, (b) MgO, and (c) γ-Al_2O_3.

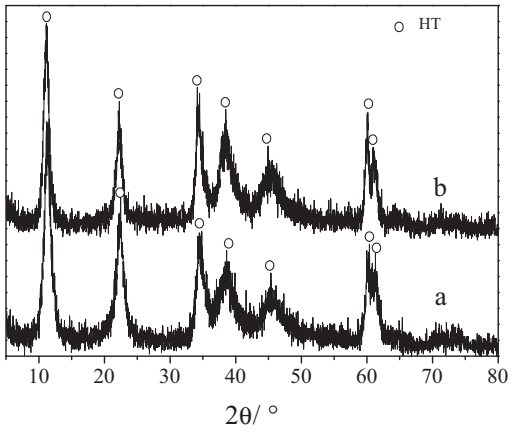

Fig. 2. XRD patterns of (a) HT and (b) Au-Pt/HT.

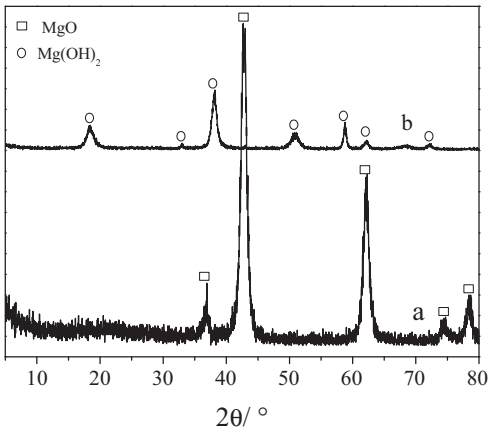

Fig. 3. XRD patterns of (a) MgO and (b) Au-Pt/MgO.

$Mg(OH)_2$ was the major phase for Au-Pt/MgO [23,24], demonstrating that MgO was rehydrated to form $Mg(OH)_2$, during the process of doping. No reflections corresponding to Au or Pt were observed for the three supported catalysts, due to the low loadings.

3.1.3. Basic sites on the surface of supports

The property of basic site is related to the state of O ions [25]. In order to investigate the state of O ions, the XPS spectra of O 1s for catalysts were determined (Fig. 5). The analyses on the three catalysts have shown the following peaks: (i) in the range of 529.8–530.4 eV, O 1s peaks characteristic of the "O^{2-}" ions of the

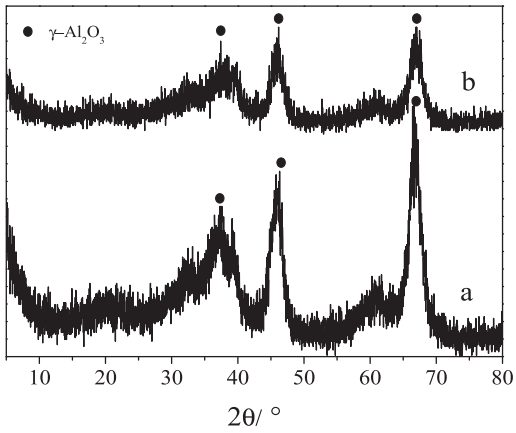

Fig. 4. XRD patterns of (a) γ-Al_2O_3 and (b) Au-Pt/γ-Al_2O_3.

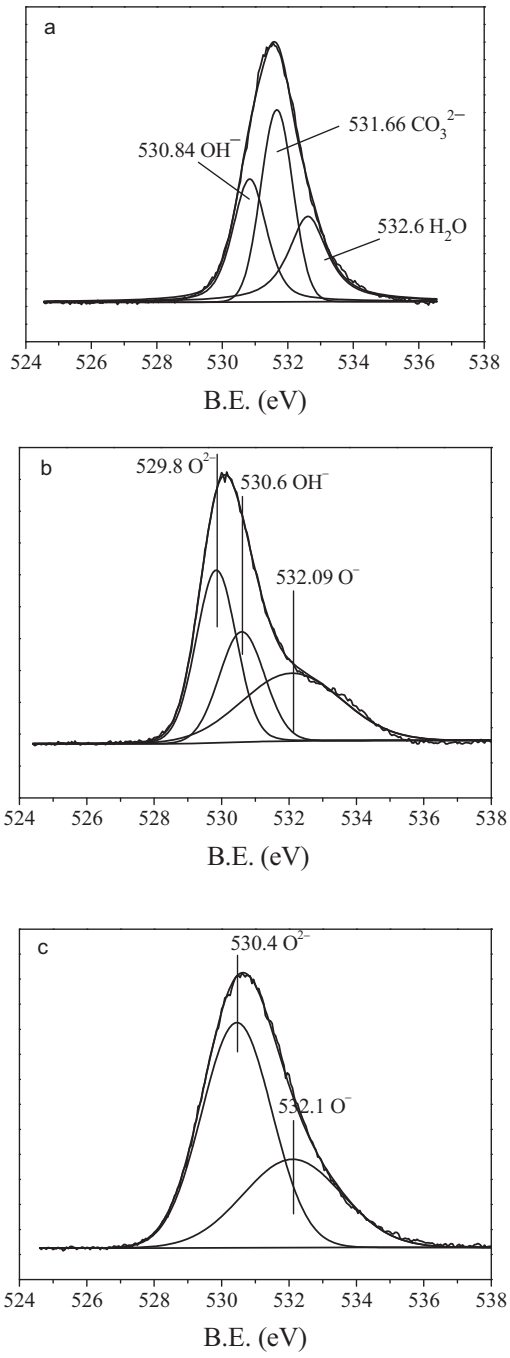

Fig. 5. O 1s XPS spectra of (a) Au-Pt/HT, (b) Au-Pt/MgO, and (c) Au-Pt/γAl_2O_3 catalysts.

crystalline network; (ii) in the range of 530.6–530.8 eV, O 1s peaks characteristic of the "OH^-" ions of the crystalline network; (iii) in 531.7 eV, O 1s peaks characteristic of the "CO_3^{2-}" ions of the crystalline network; and (iv) in the range of 531.1–531.2 eV, O 1s peaks characteristic of the "O^-" ions. The "O^-" ions are assigned to ionizations of weakly adsorbed species and also ionizations of oxygen ions with particular coordinations more specially integrated in the subsurface (bulk structure near the surface) [26]. The results indicated that oxygen had four states for the prepared catalysts. Among them, "O^-" ions did not relate to the basic property of catalysts. Apart from "O^-" ions, oxygen in the other three states contributes to the basic properties of the catalysts. On the surface of Au-Pt/HT catalyst, there were two kinds of basic sites, "OH^-" and "CO_3^{2-}" [27]. The

Table 2
Acid and basic properties of supports.

Entry	Supports	Basic strength	Acid strength
1	γ-Al_2O_3	$7.2 < H_- < 9.8$	$4.8 < H_o < 6.8$
2	HT	$9.8 < H_- < 11$	$4.8 < H_o < 6.8$
3	$Mg(OH)_2$	$9.8 < H_- < 11$	
4	MgO	$12.2 < H_- < 15$	
5	ZnO	$7.2 < H_- < 9.8$	$4.8 < H_o < 6.8$
6	$CaCO_3$	$9.8 < H_- < 11$	
7	$(MgCO_3)_4Mg(OH)_2$	$9.8 < H_- < 11$	
8	TiO_2		$3.3 < H_o < 4.8$
9	CeO_2		$3.3 < H_o < 4.8$

"OH^-" surface content normalized to the total amount of surface oxygen species was 32%, which was obtained by calculating the area of corresponding XPS peaks ($A_{OH^-}/A_{OH^-} + A_{CO_3^{2-}} + A_{H_2O} = 0.32$); and the "$CO_3^{2-}$" surface content was 39%. The surface content "OH^-" was similar to that of "CO_3^{2-}", which suggested that both "CO_3^{2-}" and "OH^-" were the main basic sites on Au-Pt/HT catalysts. For the Au-Pt/MgO catalyst, "O^{2-}" surface content was 38% and "OH^-" surface content was 26%. The coexistence of "O^{2-}" and "OH^-" demonstrated that Lewis basic sites of MgO partly transform to Brønsted basic sites of $Mg(OH)_2$ in the process of Au-Pt deposition. This also showed that the main basic sites on the Au-Pt/MgO catalyst were "O^{2-}" and "OH^-". For the Au-Pt/γ-Al_2O_3 catalyst, there was only one kind of basic site on the surface evident, i.e., "O^{2-}".

3.1.4. The strength of acid/basic sites of supports

The strength of the basic sites in the supports was analyzed qualitatively using Hammett indicators. As shown in Table 2, γ-Al_2O_3 possessed H_- values in the range $7.2 < H_- < 9.8$ (entry 1), HT and $Mg(OH)_2$ possessed H_- values in the range $9.8 < H_- < 11$ (entries 2 and 3) and the H_- values of MgO were in the range $12.2 < H_- < 15$ (entry 4). This means that MgO had the strongest basic sites, next were $Mg(OH)_2$ and HT, and γ-Al_2O_3 had the weakest basic sites.

The strength of the acid sites in the supports was also analyzed using Hammett indicators (Table 2). γ-Al_2O_3 possessed H_o values in the range $4.8 < H_o < 6.8$ (entry 1), which was similar to that of HT ($4.8 < H_o < 6.8$; entry 2). This demonstrated that the strength of acid sites on γ-Al_2O_3 was similar to that of HT. $Mg(OH)_2$ and MgO did not appear to have any acid sites (Table 2, entries 3 and 4).

Combining the results concerning the acid and base sites of the supports, it was found that γ-Al_2O_3 and HT possessed both acid and basic sites, while $Mg(OH)_2$ and MgO only contained basic sites.

The acid/base nature of the reference supports was also investigated. ZnO possessed H_- values in the range $7.2 < H_- < 9.8$ and H_o values in the range $4.8 < H_o < 6.8$ (Table 2, entry 5). This indicated that ZnO contained both acid and base sites, and their strength was similar to γ-Al_2O_3. Both $CaCO_3$ and $(MgCO_3)_4Mg(OH)_2$ contained only basic sites (Table 2, entries 6 and 7). The strength of their basic sites was in the range $9.8 < H_- < 11$, which was similar to that of $Mg(OH)_2$ or HT. In contrast, both TiO_2 and CeO_2 contained only acid sites (Table 2, entries 8 and 9) and the strength of their acid sites was in the range $3.3 < H_o < 4.8$, being lower than that of the other supports.

3.1.5. The size and composition of Au-Pt nanoparticles

The microstructure and compositions of Au-Pt nanoparticles was characterized by a STEM with EDS. The microscope was set to achieve Z contrast imaging. Large area STEM images are shown in Fig. 6. The bright area represents the Au-Pt nanoparticles and the gray and dark area corresponds to the support. The size of Au-Pt nanoparticles was similar for the different supports. It was in the range of 1.9–2.1 nm. Figs. 7–9 show the atomic resolution Z-contrast image of the Au-Pt nanoparticles on MgO, γ-Al_2O_3, and

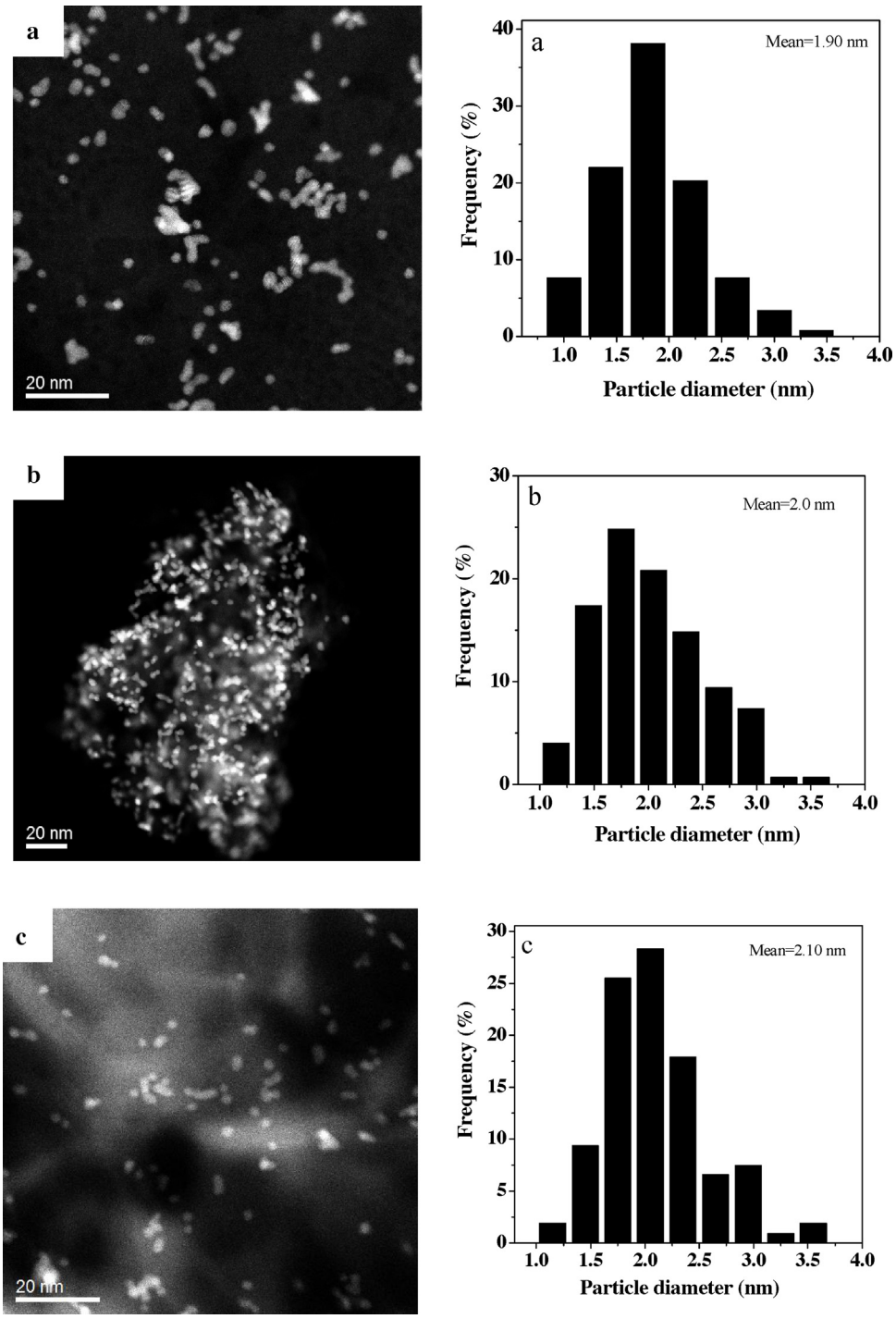

Fig. 6. STEM images and Au-Pt particle size distributions for (a) Au-Pt/MgO, (b) Au-Pt/γ-Al_2O_3, and (c) Au-Pt/HT.

HT supports, respectively. During the process of line scan, the beam damage was observed, which caused the microstructure of nanoparticles being changed slightly, but we think this effect do not change the composition of Au-Pt nanaoparticle. The EDS line scan analysis indicated the nanoparticles were homogeneously Au-Pt alloyed structure for all the supports.

3.2. *Effect of catalyst supports*

The effect of support (HT, MgO and γ-Al_2O_3) on the selectivity of products was also investigated (Table 3, entries 1–3). The detected products were GLYA, GLYALD, GLYCA, TARAC, GA, and OXALA. It was found that the supports affected the selectivity of products. Take catalysts with 1:3 Au/Pt ratios as examples. The selectivity to GLYA for Au-Pt/HT was 72% (Table 3, entry 1), next was Au-Pt/γ-Al_2O_3 (51%; Table 3, entry 3), and the lowest selectivity to GLYA came from Au-Pt/MgO (40%; Table 3, entry 2). The selectivity to GLYALD for Au-Pt/γ-Al_2O_3, Au-Pt/HT and Au-Pt/MgO were 31% (entry 3), 12% (entry 1), and 2% (entry 2), respectively. This indicated that Au-Pt/γ-Al_2O_3 had the highest selectivity to GLYALD, and Au-Pt/MgO had the lowest selectivity to it. For the other four products, GLYCA, TARAC, GA, and OXALA, the highest selectivity came from Au-Pt/MgO, next was Au-Pt/HT, and Au-Pt/γ-Al_2O_3 showed the lowest selectivity. For example, the selectivity

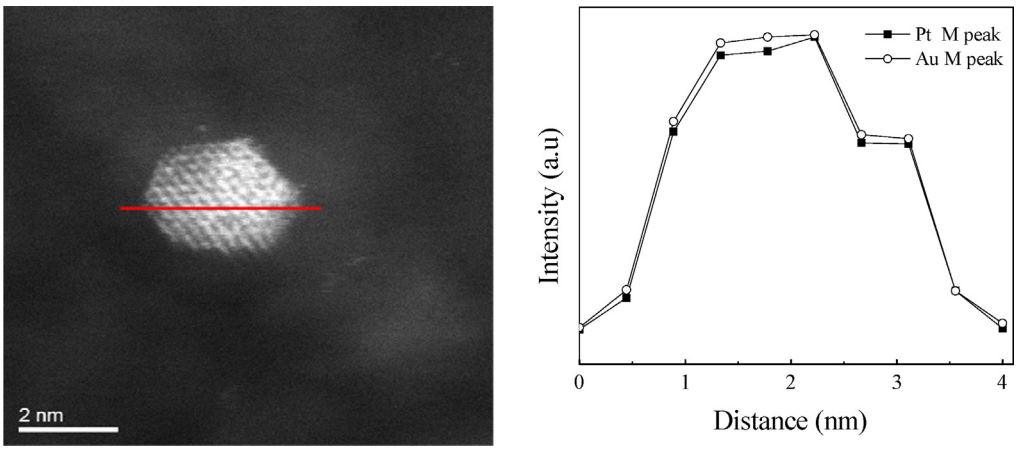

Fig. 7. (a) HADFF-STEM image of the Au-Pt/MgO nanoparticle; (b) intensity profiles of Pt(M) and Au(M) components in the nanoparticle obtained by a EDS line scan analysis (along the red line in (a) from left to right). (For interpretation of the references to color in this figure legend, the reader is referred to the web version of the article.)

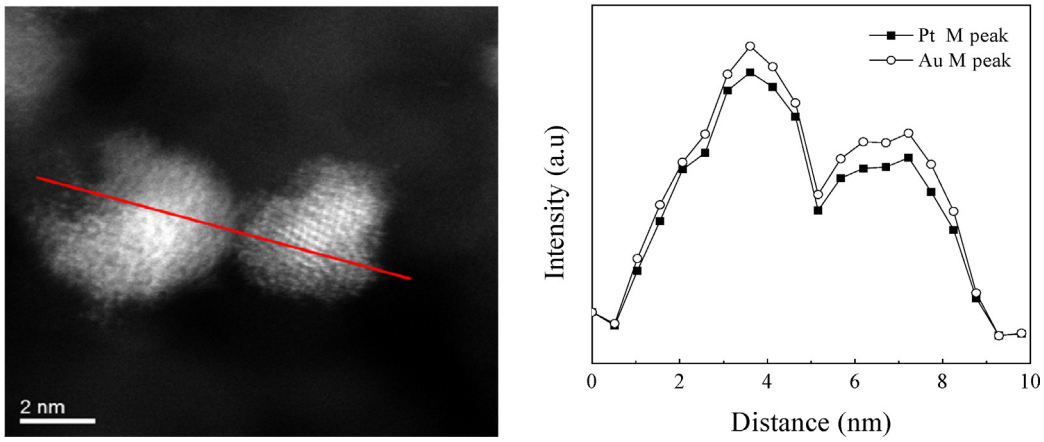

Fig. 8. (a) HADFF-STEM image of the Au-Pt/γ-Al_2O_3 nanoparticles; (b) intensity profiles of Pt(M) and Au(M) components in the nanoparticles obtained by a EDS line scan analysis (along the red line in (a) from left to right). (For interpretation of the references to color in this figure legend, the reader is referred to the web version of the article.)

to GA for Au-Pt/MgO, Au-Pt/HT, and Au-Pt/γ-Al_2O_3 was 7.5% (entry 2), 0.4% (entry 1), and 0.2% (entry 3), respectively. The effect of Au/Pt ratio was investigated and the results are shown in Table 4. It can be seen that conversion of glycerol ranged from 3% (Table 4, entry 8) to 64% (Table 4, entry 4), changing with Au/Pt ratio and type of support. However, the distribution of products was similar to that of catalysts with 1:3 Au/Pt ratios. For each Au/Pt ratio, Au-Pt/HT showed the highest selectivity to GLYA. Au-Pt/MgO had the lowest selectivity to GLYALD, and Au-Pt/γ-Al_2O_3 showed the highest selectivity to GLYALD. For 3:1 Au/Pt ratio, the selectivity to GLYA for Au-Pt/HT, Au-Pt/MgO, and Au-Pt/γ-Al_2O_3 was 82% (Table 4, entry 2), 56% (Table 4, entry 9), and 63% (Table 4, entry 16),

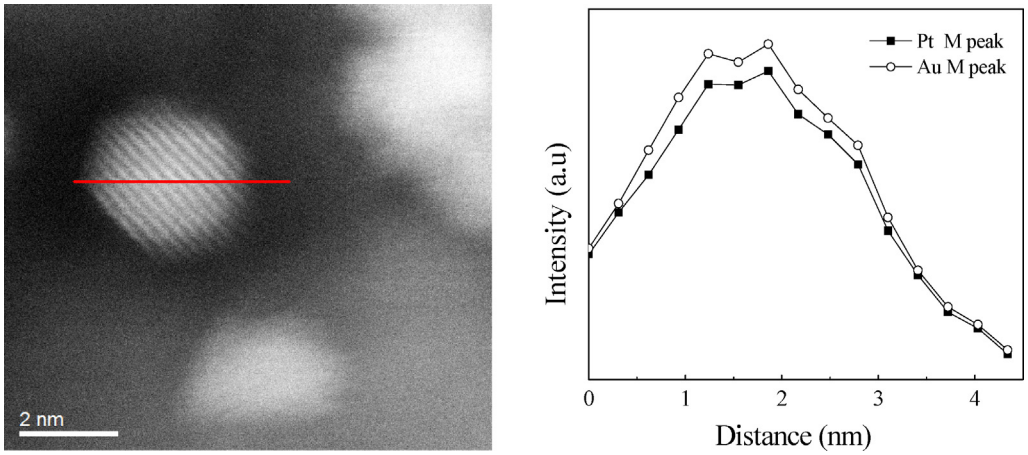

Fig. 9. (a) HADFF-STEM image of the Au-Pt/HT; (b) intensity profiles of Pt(M) and Au(M) components in the Simple obtained by a EDS line scan analysis (along the red line in (a) from left to right). (For interpretation of the references to color in this figure legend, the reader is referred to the web version of the article.)

Table 3
The effect of supports on selectivity of products (Au/Pt, 1:3).[a]

Entry	Supports	Glycerol conversion (%)	Product selectivity (%)						Mass balance (%)[a]
			GLYA	GLYALD	GLYCA	TARAC	GA	OXALA	
1	HT	57	72	12	10	5	0.4	0.5	99.9
2	MgO	45	40	2	11	11	7.5	1.1	72.6
3	γ-Al_2O_3	39	51	31	8	5	0.2	0.4	95.6
4	$Mg(OH)_2$	49	53	2	10	4	8	0.6	77.6
5	$(MgCO_3)_4Mg(OH)_2$	50	69	14	12	4	0.5	0.4	99.9
6	$CaCO_3$	43	61	20	6	4	1.0	0.1	92.1
7	ZnO	16	55	34	6	2	2.6	0.1	99.7
8	CeO_2	33	29	35	0.5	0.4	0	0	64.9
9	TiO_2	29	37	52	5	1	0	0	95

[a] Determined on the basis of observed C_2 and C_3 products.

respectively. The selectivity to GLYALD for Au-Pt/HT, Au-Pt/MgO, and Au-Pt/γ-Al_2O_3 was 8% (Table 4, entry 2), 3% (Table 4, entry 9), and 33% (Table 4, entry 16), respectively. On this basis it can be seen that the distribution of products was related to the nature of the supports, and not to the Au/Pt ratio and the conversion of glycerol. In general, the selectivity values should be compared for similar values of conversion level. In this work, the effect of conversion on the selectivity was neglected relative to that of supports.

In order to further understand the role of the nature of the support, a series of reference supports were investigated as shown in entries 4–9 of Table 3. The distribution of products on $Mg(OH)_2$ (entry 4) was similar to that on MgO (entry 2), while the distribution of products for $(MgCO_3)_4Mg(OH)_2$ (entry 5) was similar to that on HT (entry 1). For the $CaCO_3$ support (entry 6), the selectivity to GLYA (61%) was higher than that of γ-Al_2O_3 (51%), but the selectivity to GLYALD (20%) was lower than that of γ-Al_2O_3 (31%). The distribution of products for ZnO (entry 7) was similar to that for γ-Al_2O_3. Although the selectivity of products changed with supports, there is one common feature for supports from entries 1 to 7. For these supports, the main product was GLYA, the selectivity to which was higher than that to other products. However, for CeO_2 (entry 8) and TiO_2 (entry 9), the selectivity to GLYALD was higher than the selectivity to GLYA, which differed from the other supports. For example, the selectivity to GLYALD of TiO_2 was 52%, while its selectivity to GLYA was 37%.

Although glycerol oxidation produces both liquid and gas products [8], as shown in Table S2, the products of glycerol oxidation over noble metal catalysts were mainly liquid products. In this work, only the liquid products were detected. For most supports, the mass balance was greater than 90%, indicating that the main products of glycerol oxidation were liquid. This is in accordance with the references in Table S2. For example, the mass balance for Au-Pt/HT was 99.9% (Table 3, entry 1), and the mass balance for ZnO was 99.7% (Table 3, entry 7). For the nine supports, only three supports, i.e., MgO, $Mg(OH)_2$, and CeO_2, had low mass balance, which was in the range of 60–77%. The reason for the low mass balance of MgO and $Mg(OH)_2$ can be ascribed to their basic properties as discussed below. CeO_2 is redox active [28,29] and the changeable valence of Ce may affect the mass balance. The reason for its low mass balance will be investigated in the future work.

3.3. Combination of acid/basic property of supports with the distributions of products

Considering the selectivity of products in relation to the supports, it was found that the distribution of products was related to their acid/base nature. Acid sites promoted the formation of GLYALD, while base sites lowered the selectivity to GLYALD. In other words, the selectivity to GLYALD was proportional to the acid strength of supports, but inversely proportional to the basic strength of supports. Among the three supports, i.e. HT, MgO, and γ-Al_2O_3, MgO had the strongest basic sites, while the basic sites on surface of γ-Al_2O_3 were the weakest. This explained the lowest selectivity to GLYALD by Au-Pt/MgO and the highest one by Au-Pt/γ-Al_2O_3. This suggestion was further supported by the

Table 4
The effect of supports and Au/Pt ratio on selectivity of products.

Entry	Catalyst (Au/Pt ratio)	Glycerol conversion (%)	Product selectivity (%)					
			GLYA	GLYALD	GLYCA	TARAC	GA	OXALA
1	Au/HT	6	67	15	13	0	0	0
2	Au-Pt/HT (3:1)	35	82	8	4	4	0.3	0.9
3	Au-Pt/HT (1:1)	44	72	13	7	5	0.4	1.1
4	Au-Pt/HT (1:5)	64	69	12	12	4	0.7	1.2
5	Au-Pt/HT (1:7)	60	70	13	11	3	0.7	1.6
6	Au-Pt/HT (1:9)	45	62	20	9	2	0.5	1.2
7	Pt/HT	44	66	20	11	1	0.6	0.6
8	Au/MgO	3	50	2	6	20	0	0
9	Au-Pt/MgO (3:1)	34	56	3	12	10	7	1.4
10	Au-Pt/MgO (1:1)	52	48	4	11	9	10	1.3
11	Au-Pt/MgO (1:5)	45	40	2	11	11	10.9	1.9
12	Au-Pt/MgO (1:7)	35	40	3	14	11	11.7	1.7
13	Au-Pt/MgO (1:9)	33	36	3	12	9	11.3	1.5
14	Pt/MgO	29	34	3	14	10	11	1.2
15	Au/γ-Al_2O_3	5	27	62	0	2	0	0
16	Au-Pt/γ-Al_2O_3 (3:1)	11	63	33	1	2	0	0
17	Au-Pt/γ-Al_2O_3 (1:1)	26	65	27	4	3	0.07	0
18	Au-Pt/γ-Al_2O_3 (1:5)	37	54	30	5	4	0.2	0.8
19	Au-Pt/γ-Al_2O_3 (1:7)	36	57	33	5	3	0.2	0.9
20	Au-Pt/γ-Al_2O_3 (1:9)	28	50	39	3	2	0.04	0.2
21	Pt/γ-Al_2O_3	20	50	45	0	0	0	0

results of the other reference supports. The acid strength of $CaCO_3$ was lower than that of γ-Al_2O_3. Similarly, its selectivity to GLYALD was also lower. The base site strength of ZnO was similar to that of γ-Al_2O_3. Its selectivity to GLYALD was also similar. The acid site strengths of CeO_2 and TiO_2 were higher than that of γ-Al_2O_3. Their selectivity to GLYALD was also higher. The acid strength of CeO_2 and TiO_2 was so strong that their selectivity to GLYALD was higher than their selectivity to GLYA, resulting in their main product being GLYALD and not GLYA.

TARAC is produced by the sequential oxidation of GLYA, while GLYCA is the product of sequential oxidation of TARAC (Scheme 1). The sequential oxidation of GLYCA generates GA, and sequential oxidation of GA generates OXALA. For the four products, Au-Pt/MgO, which had the strongest basic sites, showed the highest selectivity; while Au-Pt/γ-Al_2O_3, containing the weakest basic sites, displayed the lowest selectivity. This indicated that the selectivity to TARAC, GLYCA, GA, and OXALA were proportional to the strength of base site on supports, and that the strength of base site on supports promoted the sequential oxidation of GLYA, TARAC, GLYCA, GA, and OXALA. This suggestion was also supported by the results of the reference supports. The base site strengths of CeO_2 and TiO_2 supports were the weakest. Their selectivity to TARAC (<1%) was also the lowest. The strengths of the base site of MgO support were the strongest. Their selectivity to TARAC (11%) was also the highest. The above analysis showed that the selectivity to GLYALD was inversely proportional to the strength of basic sites of supports, and the selectivity of GLYCA, TARAC, GA, and OXALA was proportional to the strength of basic sites of supports. Next, consider the relationship between the selectivity to GLYA and the nature of basic sites on supports.

The selectivity to GLYA was neither proportional to the strength of the base sites of the supports nor proportional to the strength of the acid sites of the supports. For HT, MgO, and γ-Al_2O_3, HT had the highest selectivity to GLYA. However, the basic strength of HT was lower than that of MgO, and its acid strength was similar to that of γ-Al_2O_3. There were two types of base sites and one acid site on surface of HT. The base sites were Mg-OH^- and Mg-CO_3^{2-}, and acid site was Al-OH^-. Its high selectivity to GLYA may be related to its acid/base properties. There were two possible reasons for its high selectivity to GLYA. One possible reason is a synergistic effect of acid sites and base sites and their coexistence may contribute to the formation of GLYA. Au-Pt/γ-Al_2O_3 and Au-Pt/HT contained both acid and basic sites, which explained their high selectivity to GLYA. In the case of the coexistence of acid and base sites, the selectivity to GLYA was affected by the strength of the base sites. Au-Pt/γ-Al_2O_3 and Au-Pt/HT differed in the strength of their base sites, which accounted for their different in selectivity to GLYA. Another possible reason was the effect of the Mg-CO_3^{2-} base sites. In order to investigate the effect of the Mg-CO_3^{2-} base sites, Au-Pt/$(MgCO_3)_4Mg(OH)_2$ was tested. The $(MgCO_3)_4Mg(OH)_2$ support was similar to HT in terms of the presence of Mg-OH^- and Mg-CO_3^{2-} base sites. The distribution of products for Au-Pt/$(MgCO_3)_4Mg(OH)_2$ (Table 3, entry 5) was also similar to that of Au-Pt/HT (Table 3, entry 1). This indicated that the possible reason for the high selectivity to GLYA of Au-Pt/HT was the coexistence of Mg-OH^- and Mg-CO_3^{2-} basic sites. For the two reasons above, which one was more important? The literature suggests that the synergistic effect of acid sites and basic sites are the main reason for the unique catalytic property of HT supports in alcohol oxidation [30]. However, in this work, the results for Au-Pt/$(MgCO_3)_4Mg(OH)_2$ suggested that the existence of Mg-CO_3^{2-} base sites could not be neglected. Analyzing the Al-OH^- acid sites and Mg-CO_3^{2-} base sites on the surface of HT, it was found that there was one common feature between these two sites. Each of the two sites (Al-OH^- acid sites or Mg-CO_3^{2-} basic sites) resulted in the fact that the strong basic site of Mg-OH^- was mixed with another weak basic site. The doping of another weak basic site may result in the high selectivity to GLYA.

In order to further investigate the effect of the doping of another weak basic site, Au-Pt/MgO (Table 3, entry 2) and Au-Pt/$Mg(OH)_2$ (Table 3, entry 4) were investigated. Au-Pt/MgO contained both Mg-O^{2-} and Mg-OH^-, while Au-Pt/$Mg(OH)_2$ only contained Mg-OH^-. Their distribution of products was similar. The selectivity to GLYALD (2%) was the lowest amongst the supports investigated. The selectivity to GLYA was lower than that of both Au-Pt/HT and Au-Pt/γ-Al_2O_3. Their mass balance of products for each of Au-Pt/MgO and Au-Pt/$Mg(OH)_2$ was the lowest amongst the supports investigated. TARAC, GLYCA, GA, and OXALA are products of the over oxidation of GLYA. They are all acid products. The reason for the over oxidation is that the acid products formed are strongly bound to the support (base) and most of them will not desorb until they are further oxidized to CO_2. This is also the reason for the poor mass balance by MgO and $Mg(OH)_2$. MgO and $Mg(OH)_2$, which had strong basic sites, could bind the acid products strongly and promote over-oxidation of GLYA effectively; whereas the strength of basic sites on $MgCO_3$ and Al_2O_3 was too low to facilitate the over-oxidation of GLYA. The doping of basic sites Mg-CO_3^{2-} and acid sites Al-OH^- decreased the density of Mg-OH^- on the surface of HT. The decrease in the density of Mg-OH^- promoted the desorption of acid products and restrained the over-oxidation of GLYA. Combining the above discussion about effect of acid/base properties of supports on the selectivity to other products (i.e., GLYALD, TARAC, GLYCA, GA, and OXALA), the relationship between the selectivity of glycerol oxidation and acid/basic nature of supports is outlined in Scheme 2. In Scheme 2, each reaction was denoted by one number. For example, the reaction of glycerol oxidized to GLYALD was denoted (1), and the reaction of GLYALD oxidized to GLYA was denoted (2). Because all the supports, whether basic or acid, could catalyze reaction (1), it suggested that reaction (1) occurred irrespective of the acid/base nature of supports. Reaction rates of reactions (2)–(6), i.e., sequential oxidation of GLYALD to GLYA, TARAC, GLYCA, GA, and OXALA, were proportional to the strength of basic sites on supports.

Based on Scheme 2, the above question about the effect of supports on selectivity to GLYA can be answered well. Glycerol is oxidized by oxygen to form GLYALD (reaction (1)). GLYALD participated in a series of over oxidation reactions, i.e., reactions (2)–(6). The rate of reactions (1)–(6) affected the relative amounts of products. The amount of GLYA was affected by the relative reaction rate of reactions (2) and (3). The increase of reaction rate of reactions (2) would increase the amount of GLYA, whereas the increase of reaction rate of reactions (3) would decrease the amount of GLYA. The reaction rate of reactions (2)–(6) was affected by the acid/basic property of supports. Mg-OH^- sites were present on HT. Mg-OH^- could catalyze both reactions (2) and (3) effectively. The doping of basic sites Mg-CO_3^{2-} and acid sites Al-OH^- decreased the reaction rate of reaction (3), but had little effect on the rate of reaction (2). Accordingly, the selectivity to GLYA was increased by introducing Mg-CO_3^{2-} base sites or Al-OH^- acid sites. This introduction also decreased reaction rate of reactions (4)–(6). Therefore, HT showed the highest selectivity to GLYA. Similar to the basic property of HT, the base site Mg-OH^- of $(MgCO_3)_4Mg(OH)_2$ was also replaced by another weaker basic site of Mg-CO_3^{2-}. So, $(MgCO_3)_4Mg(OH)_2$ also showed high selectivity to GLYA. Among the supports investigated, MgO or $Mg(OH)_2$ showed the highest basic strength. Furthermore, the base sites of MgO or $Mg(OH)_2$ were not substituted by a weaker basic site. Therefore, reactions (2)–(6) could be catalyzed well. The increase of reaction rate of reactions (2)–(6) would decrease the amount of GLYALD. This explained why MgO or $Mg(OH)_2$ showed the lowest selectivity to GLYALD. On the

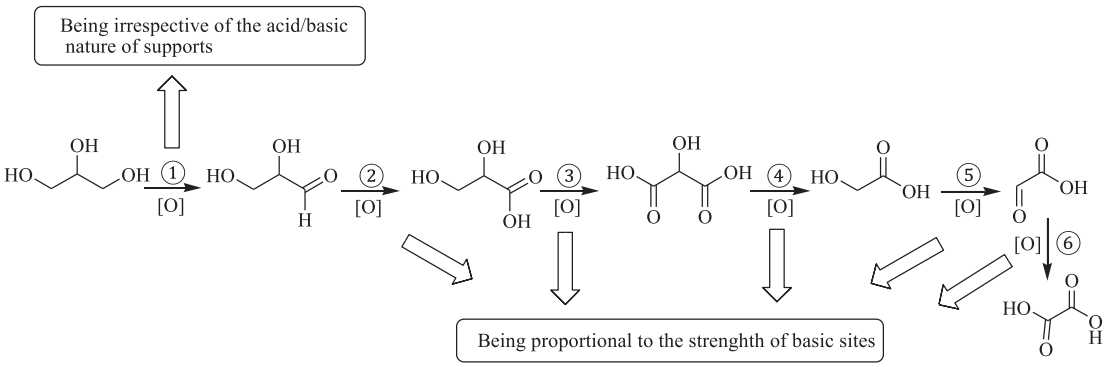

Scheme 2. Relationship between acid/basic nature of supports and reaction rates.

other hand, the increase of reaction rates of reactions (3)–(6) would also decrease the amount of GLYA. This explained why MgO or $Mg(OH)_2$ showed lower selectivity to GLYA than HT did. With similar considerations, the distribution of products by other supports could be correlated with their corresponding acid/base nature. For example, TiO_2 had the weakest basic sites. The weakest basic sites limited the reaction rate of reactions (2)–(6). The decrease in reaction rate of reactions (2)–(6) would increase the relative amount of GLYALD, explaining why TiO_2 had the highest selectivity to GLYALD.

4. Conclusion

In this work, the effect of acid/basic nature of supports on the aerobic oxidation of glycerol over supported Au-Pt bimetallic catalysts was studied in detail. It was found that the distribution of products was affected by the acid/base nature of the catalyst supports. The doping of another weaker basic site promoted the desorption of acid products, restrained the over-oxidation of GLYA, and increased the selectivity to GLYA. The reaction rate of glycerol oxidized to GLYALD (reaction (1)) was irrespective of the acid/base nature of supports. Reaction rates of reaction (2) to (6), i.e., sequential oxidation of GLYALD to GLYA, TARAC, GLYCA, GA, and OXALA, were proportional to the strength of basic sites on supports. MgO, which had the strongest basic sites, showed the lowest selectivity to GLYALD, but the highest selectivity to TARAC, GLYCA, GA, and OXALA. HT, where the strong basic site of Mg-OH^- was replaced with other weak basic sites (Al-OH^- acid sites or Mg-CO_3^{2-} basic sites), displayed the highest selectivity to GLYA. The replacement of weak basic sites decreased both the density of the Mg-OH^- base sites and reaction rate of reaction (3), which resulted in it having the highest selectivity to GLYA. TiO_2, which had the weakest basic sites, had the highest selectivity to GLYALD.

Acknowledgements

This work was supported by the projects funded by National Natural Science Foundation of China (Program No. 21343015) and by the Fundamental Research Funds for the Central Universities (Program No. GK201302016).

Appendix A. Supplementary data

Supplementary data associated with this article can be found, in the online version, at http://dx.doi.org/10.1016/j.apcatb.2014.09.048.

References

[1] H. Kopetz, Nature 494 (2013) 29.
[2] J. Colmenares, R. Luque, Chem. Soc. Rev. 43 (2014) 765.
[3] P. Gallezot, Chem. Soc. Rev. 41 (2012) 1538.
[4] C.D. Pina, E. Falletta, M. Rossi, Chem. Soc. Rev. 41 (2012) 350.
[5] S.E. Davis, M.S. Ide, R.J. Davis, Green Chem. 15 (2013) 17.
[6] A. Arcadi, Chem. Rev. 108 (2008) 3266.
[7] B.N. Zope, S.E. Davis, R.J. Davis, Top. Catal. 55 (2012) 24.
[8] C. Zhou, J.N. Beltramini, C. Lin, Z. Xu, G.Q. (Max) Lu, A. Tanksale, Catal. Sci. Technol. 1 (2011) 111.
[9] A. Villa, G.M. Veith, L. Prati, Angew. Chem. Int. Ed. 49 (2010) 4499.
[10] S. Carrettin, P. McMorn, P. Johnston, K. Griffin, G.J. Hutchings, Chem. Commun. (2002) 696.
[11] L. Prati, P. Spontoni, A. Gaiassi, Top. Catal. 52 (2009) 288.
[12] G.L. Brett, Q. He, C. Hammond, P.J. Miedziak, N. Dimitratos, M. Sankar, A.A. Herzing, M. Conte, J.A. Lopez-Sanchez, C.J. Kiely, D.W. Knight, S.H. Taylor, G.J. Hutchings, Angew. Chem. Int. Ed. 50 (2011) 10136.
[13] D. Tongsakul, S. Nishimura, K. Ebitani, ACS Catal. 3 (2013) 2199.
[14] A. Villa, A. Gaiassi, I. Rossetti, C.L. Bianchi, K. Benthem, G.M. Veith, L. Pratia, J. Catal. 275 (2010) 108.
[15] K.N. Heck, B.G. Janesko, G.E. Scuseria, N.J. Halas, M.S. Wong, ACS Catal. 3 (2013) 2430.
[16] J.R. Copeland, I.A. Santillan, S.M.N. Schimming, J.K. Ewbank, C. Sievers, J. Phys. Chem. C 117 (2013) 21413.
[17] C. Xu, J. Sun, B. Zhao, Q. Liu, Appl. Catal. B 99 (2010) 111.
[18] D. Liang, J. Gao, H. Sun, P. Chen, Z. Hou, X. Zheng, Appl. Catal. B 106 (2011) 423.
[19] S. Carrettin, P. McMorn, P. Johnston, K. Griffin, C.J. Kiely, G.J. Hutchings, Phys. Chem. Chem. Phys. 5 (2003) 1329.
[20] A. Tsuji, K.T.V. Rao, S. Nishimura, A. Takagaki, K. Ebitani, ChemSusChem 4 (2011) 542.
[21] N. Dimitratos, C. Messi, F. Porta, L. Prati, A. Villa, J. Molecul, Catal. A: Chem. 256 (2006) 21.
[22] H. Habe, Y. Shimada, T. Yakushi, H. Hattori, Y. Ano, T. Fukuoka, D. Kitamoto, M. Itagaki, K. Watanabe, H. Yanagishita, K. Matsushita, K. Sakaki, Appl. Environ. Microbiol. 75 (2009) 7760.
[23] C. Jia, Y. Liu, H. Bongard, F. Schüth, J. Am. Chem. Soc. 132 (2010) 1520.
[24] M.A. Brown, Y. Fujimori, F. Ringleb, X. Shao, F. Stavale, N. Nilius, M. Sterrer, H. Freund, J. Am. Chem. Soc. 133 (2011) 10668.
[25] H. Hattori, Chem. Rev. 95 (1995) 537.
[26] J. Dupin, D. Gonbeau, P. Vinatier, A. Levasseur, Phys. Chem. Chem. Phys. 2 (2000) 1319.
[27] J. Chen, Y. Song, D. Shan, E.H. Han, Corros. Sci. 53 (2011) 3281.
[28] J. Guzman, S. Carrettin, A. Corma, J. Am. Chem. Soc. 127 (2005) 3286.
[29] J. Zhang, G. Chen, M. Chaker, F. Rosei, D. Ma, Appl. Catal. B 132–133 (2013) 107.
[30] W. Fang, J. Chen, Q. Zhang, W. Deng, Y. Wang, Chem. Eur. J. 17 (2011) 1247.